ELSEVIER

Journal of Alloys and Compounds 239 (1996) 117–123

Journal of ALLOYS AND COMPOUNDS

Ordering phenomena and demixing in the quasiternary system $HgTe/CdTe/In_2Te_3$

Detlev Weitze, Heinrich M. Schmidtke, Volkmar Leute*

Institut für Physikalische Chemie der Universität Münster, Schlossplatz 4, D-48149 Münster, Germany

Received 22 February 1996

Abstract

The phase diagram of the quasiternary system $Cd_{(3-3k_2-3k_1)}Hg_{3k_1}In_{2k_2}Te_3$ for the temperature range $600 \leq T/K \leq 900$ was investigated by X-ray diffraction, DTA measurements, and electron microprobe analysis. It is shown that ordered structures are formed at special concentrations of structural vacancies. Depending on temperature and concentration, continuous order–disorder transitions could be detected. Besides spinodal miscibility gaps there also occur structural miscibility gaps and several three-phase regions.

Keywords: Ordered phases; Phase diagrams; Phase transitions; Solid solutions; Structural vacancies; Thermodynamics

1. Introduction

The three binary components HgTe, CdTe and In_2Te_3 all crystallize in the zincblende lattice, but in In_2Te_3 each third site in the cationic sublattice is vacant. These unoccupied sites in the zincblende lattice are called structural vacancies, $\underline{V}$. Solid solutions, formed from these three components, can be described by the expression $Cd_{(3-3k_2-3k_1)}Hg_{3k_1}In_{2k_2}\underline{V}_{k_2}Te_3$ where $k_2 = x_{In_2\underline{V}Te_3}$ and $k_1 = x_{Hg_3Te_3}$ are the molar fractions respectively of In_2Te_3 and Hg_3Te_3. The molar fraction k_3 of Cd_3Te_3 is given by $(1-k_2-k_1)$. The equivalent description $(Cd_{(1-y)}Hg_y)_{3(1-k_2)}In_{2k_2}\underline{V}_{k_2}Te_3$ uses the ratio $y = k_1/(k_1+k_3)$ instead of the molar fraction k_1. In the following the specification of the structural vacancies in the formulas will be omitted.

As shown in preceding papers [1–3], the structural vacancies give rise to ordering processes at special compositions, for example at $k_2 = 3/8$, $k_2 = 3/4$ and $k_2 = 1$. We will investigate the extension of the ordered phases and the disordered solid solutions with regard to dependence on temperature and composition.

2. Experiments

2.1. Preparation conditions

The binary compounds HgTe, CdTe and In_2Te_3 were synthesized from the elements (purity of Cd, Hg and In 99.999%) in evacuated quartz ampoules. Tellurium (purity 99.99%) was previously purified by distillation. CdTe was purified by repeated sublimation in dynamic vacuum.

To investigate the phase equilibria in the system $Cd_{(3-3k_2-3k_1)}Hg_{3k_1}In_{2k_2}Te_3$, a set of powder mixtures of different molar ratios of the pure binary components was prepared. These mixtures were annealed in evacuated sealed quartz ampoules until thermodynamic equilibrium was attained. Subsequently the samples were quenched in ice-water. Annealing temperatures ranged between 600 and 900 K, annealing times between 30 and 280 days.

2.2. X-ray diffraction measurements and microprobe analysis

Guinier X-ray measurements on quenched samples were used to determine the phase diagram. Homogeneous samples with an overall composition belonging to a one-phase region of the phase diagram show one of the five X-ray patterns of Fig. 1. Samples with an

* Corresponding author.

PII S0925-8388(96)02287-6

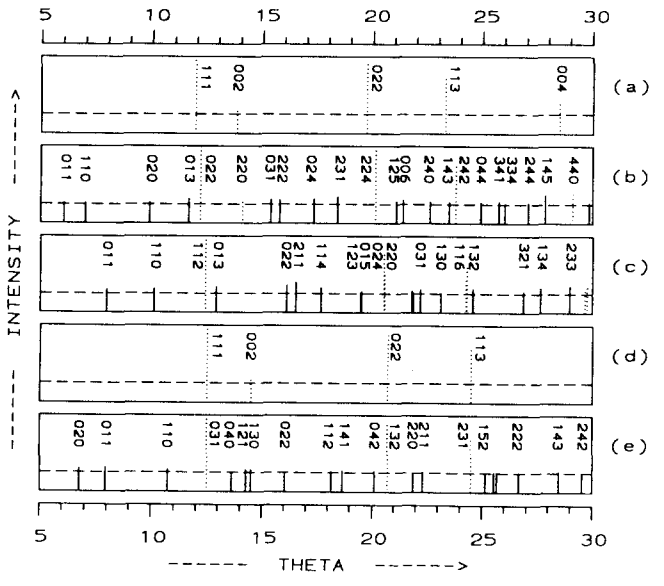

Fig. 1. X-ray patterns of homogeneous solid solutions of type $Cd_{(3-3k_2-3k_1)}Hg_{3k_1}In_{2k_2}Te_3$ with different structures: (a) HgTe (cub), (b) $Hg_5In_2Te_8$ (tet1), (c) $HgIn_2Te_4$ (tet2), (d) In_2Te_3 (cub), (e) In_2Te_3 (orh). Dotted lines: "zincblende" reflections, solid lines: superstructure reflections. The horizontal dashed lines indicate the zero level of X-ray intensity.

overall composition situated within one of the two- or three-phase regions, however, show X-ray patterns with a superposition of reflections due to the corresponding equilibrium structures (Fig. 2). For example, the pattern 2(c) represents a sample in which a CdTe-rich cubic phase is in equilibrium with a phase having tetragonal chalcopyrite structure.

The first reflection pattern (a) in Fig. 1 corresponds to that of the zincblende lattice (cub), the second (b) to that of the tetragonal superstructure at $k_2 = 0.375$ (tet1). Samples with an In_2Te_3 molar fraction near $k_2 = 0.75$ show the third reflection pattern (c) corresponding to the chalcopyrite structure (tet2). The fourth pattern (d) in Fig. 1 corresponds to the defect zincblende lattice of disordered In_2Te_3, and the last pattern (e) shows the reflections of the ordered orthorhombic In_2Te_3 structure (orh).

All patterns shown in Fig. 1 contain the reflections of the basic "zincblende" lattice. Thus, it is possible to also assign a so-called pseudo-cubic lattice constant a^* to the samples with superstructure reflections ($a_{tet1} = \sqrt{2}a^*$, $c_{tet1} = 2a^*$; $a_{tet2} = a^*$, $c_{tet2} \approx 2a^*$; $a_{orh} = a^*$, $b_{orh} = a^*/\sqrt{2}$, $c_{orh} = 3a^*/\sqrt{2}$). In the case of distorted chalcopyrite lattices with a lattice constant ratio $c/a \neq 2$, the pseudo-cubic lattice constant will be defined as $a^* = (a^2c/2)^{1/3}$.

The composition dependence of the cubic lattice constant in the quasiternary system $Cd_{(3-3k_2-3k_1)}Hg_{3k_1}In_{2k_2}Te_3$ can be described by two relations which are linear in the molar fractions k_1 and k_2. Relation I holds for small In_2Te_3 concentrations, $0 \leq k_2 \leq 0.5$, relation II for high In_2Te_3 concentrations, $0.75 \leq k_2 \leq 1$:

$$a^*(k_1, k_2)/\text{pm} = A + Bk_1 + Ck_2 + Dk_1k_2 \quad (1)$$

with I: $A = 648.40$ pm, $B = -1.77$ pm, $C = -33.55$ pm, $D = -5.42$ pm; II: $A = 641.60$ pm, $B = -6.98$ pm, $C = -24.94$ pm, $D = -0.48$ pm. Fig. 3 shows curves for constant values of the cubic lattice constant, projected onto the composition triangle ($k_2 = f(k_1)$). We call these curves "isolattice constant lines".

The difference between measured and calculated lattice constants never exceeds ±0.4 pm for all investi-

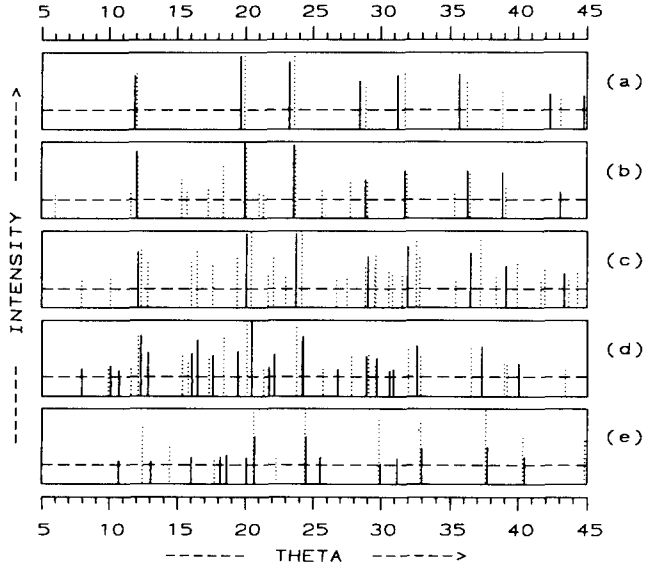

Fig. 2. X-ray patterns of ternary heterogeneous two-phase samples with different compositions (k_1, k_2): (a) (0.1, 0.2) (cub/cub), (b) (0.56, 0.3) (cub/tet1), (c) (0.08, 0.6) (cub/tet2), (d) (0.4, 0.45) (tet1/tet2), (e) (0.0375, 0.925) (tet2/orh).

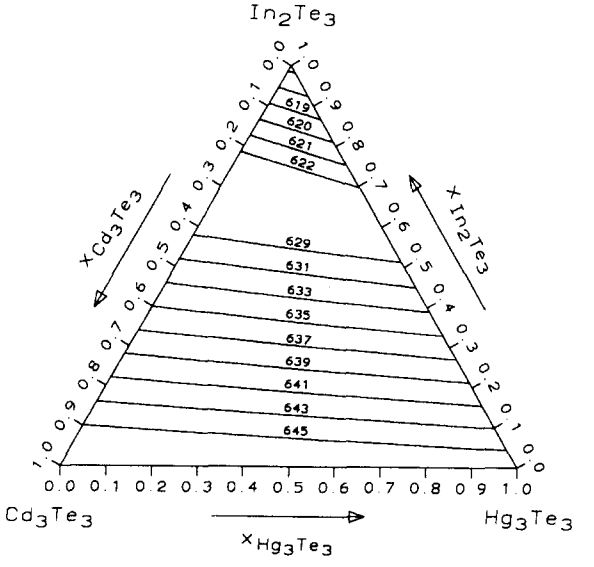

Fig. 3. Isolattice constant lines $k_2 = f(k_1)$. The numbers on the lines give the lattice constants (pm) for each of the lines ($k_1 = x(Hg_3Te_3)$), ($k_2 = x(In_2Te_3)$).

gated homogeneous samples with compositions widely spread within the regions of solubility (cf. Fig. 4(a)).

If, for a two-phase sample (α/β), the pseudo-cubic lattice constants $(a^*)_\alpha$ and $(a^*)_\beta$ for both phases were calculated from the X-ray patterns, one can determine from the relations given above the corresponding "isolattice constant lines" in Fig. 3. Thus, if for the same sample in addition the direction of the equilibrium tie-line through the point of its overall composition is known from other independent measurements, the corresponding equilibrium compositions of the two phases are obtained as the points of intersection of this tie-line with the two isolattice constant lines.

As to the directions of equilibrium tie-lines, they can be determined by an electron microprobe analysis

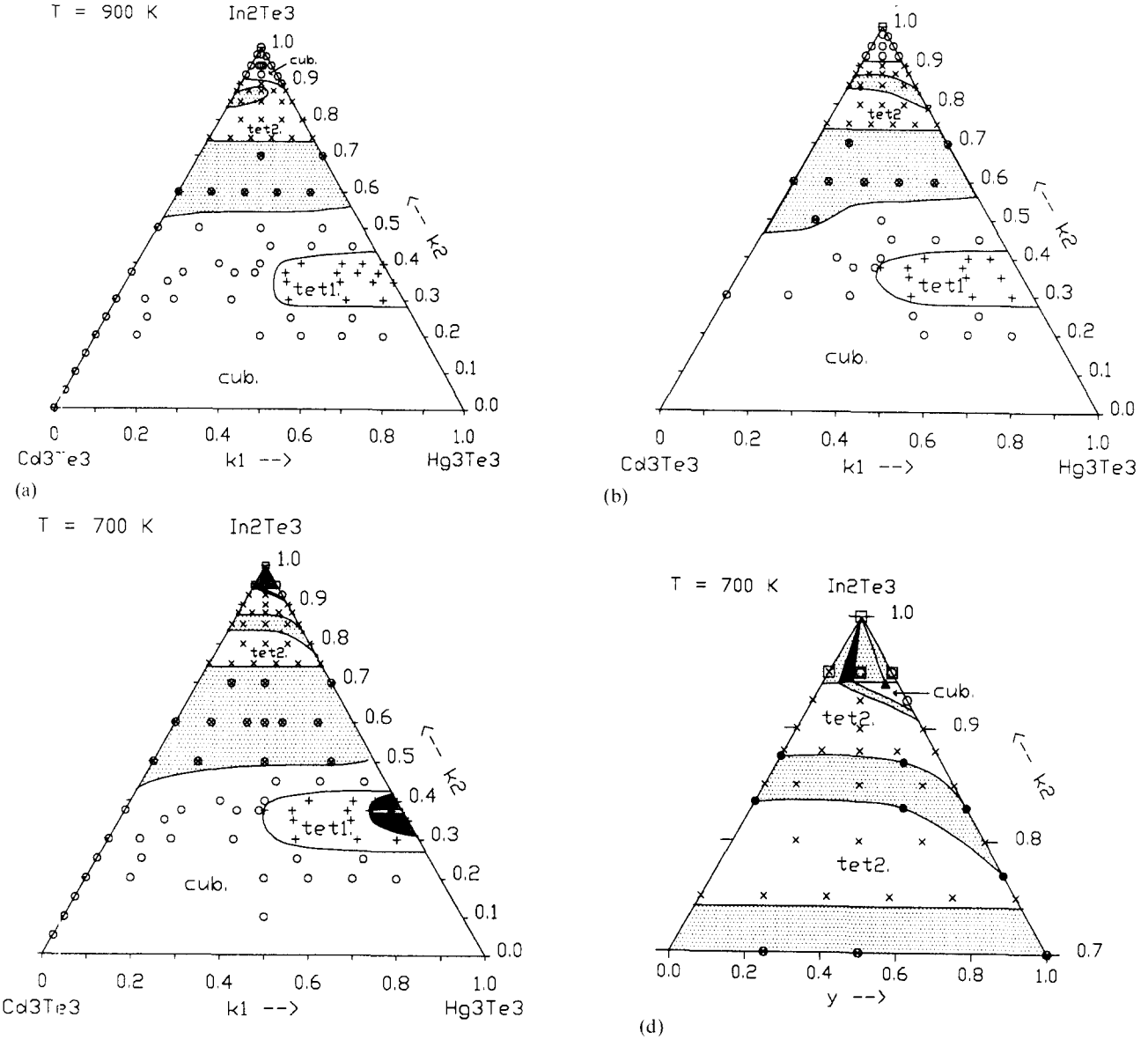

Fig. 4. Isothermal sections of the phase diagram for the quasiternary system $Cd_{(3-3k_2-3k_1)}Hg_{3k_1}In_{2k_2}Te_3$ as derived from the measurements for $T = 900$ (a), 800 (b), 700 (c,d) and 600 K (e,f,g). Widely dotted areas correspond to two-phase regions, densely dotted areas to three-phase regions. The following symbols correspond to the overall composition of samples that were homogeneous or heterogeneous after equilibration: ○, with one cubic set of reflections; +, with a tetragonal set (tet1); ×, with a tetragonal set (tet2); □, with an orthorhombic set; ⊙, with two cubic sets The superposition of two different symbols at one site indicates that the corresponding samples are two-phase samples showing the line sets of both phases. Data determined from X-ray intensity profiles taken with an electron microprobe: (a)–(d), ● characterizes tie-line end points; (d), ▲ indicates the boundary composition of the (cub/orh) two-phase region as determined from electron microprobe measurements; (f), data from spot measurements with an electron microprobe – large symbols, overall compositions of the heterogeneous samples; small symbols, scattered composition values determined at many random dots on the surface of the annealed sample. Straight lines through the dot clouds determine tie-line directions for the corresponding miscibility gap. (g), Tie-lines as determined from X-ray diffraction measurements on two-phase samples: large open symbols, overall compositions of the heterogeneous samples, small full symbols, composition values derived from the calculated lattice constants by use of the isolattice constant lines of Fig. 3 and the tie-line directions of (f).

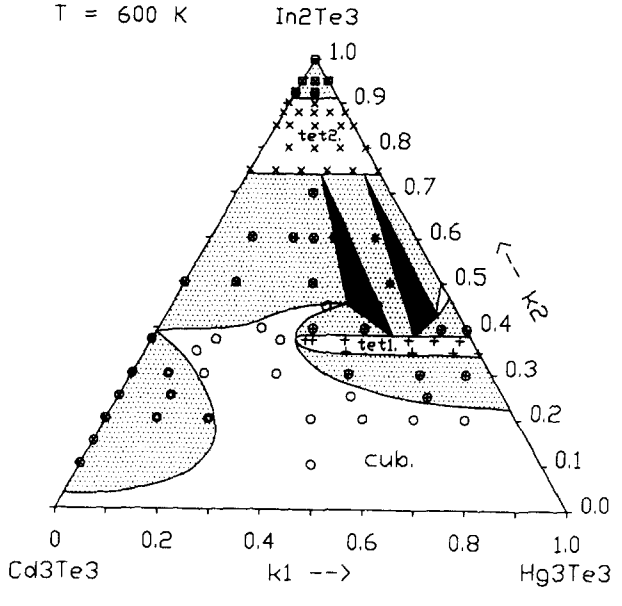

(e)

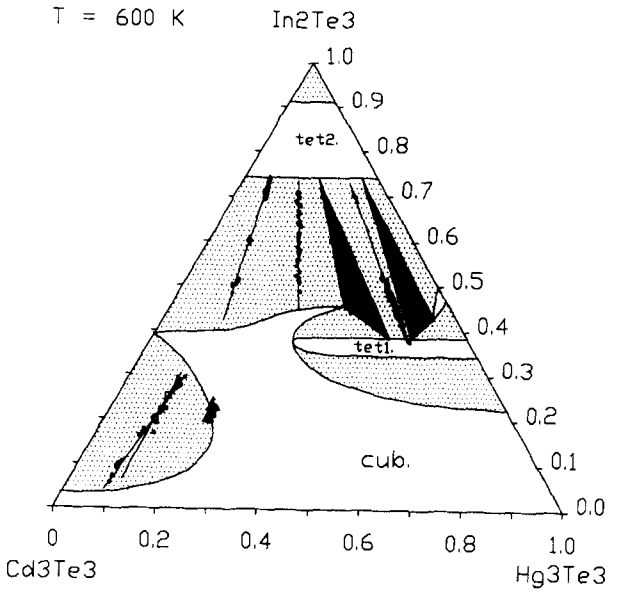

(f)

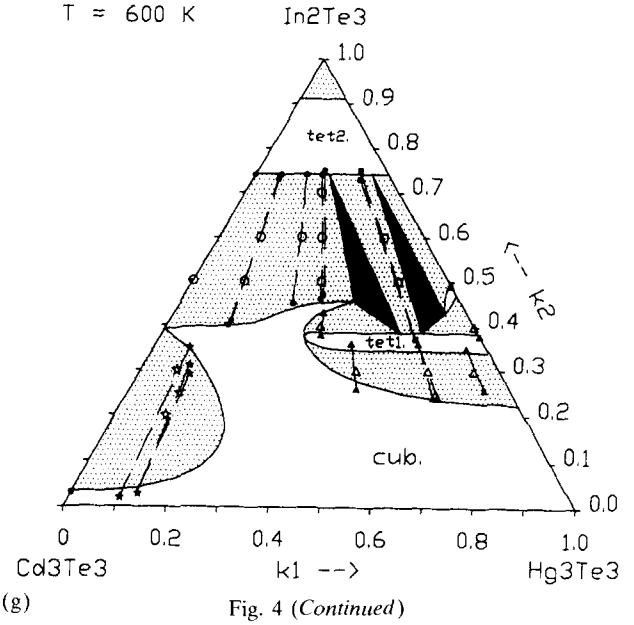

(g)

Fig. 4 (*Continued*)

of the two-phase samples. In many cases, however, the extensions of the homogeneous regions within a two-phase sample are too small to allow an exact determination of the equilibrium compositions. In such cases we determine at many points on the surface of the two-phase samples the X-ray intensities for at least two of the cationic components Cd, Hg or In. The composition points (k_1, k_2), as calculated from these intensities, are plotted in the composition triangle. As a rule they are concentrated near the requested equilibrium tie-line and a straight line, calculated by a least-squares fit through the cloud of these composition points, yields the direction of the tie-line (cf. Fig. 4(f)). The points describing the exact equilibrium compositions are situated on this straight line near the border of the cloud of composition points.

Three-phase regions can be determined in an analogous manner. In this case the cloud of composition points measured by the electron microprobe analysis is situated inside the triangle that describes the three-phase region.

2.3. DTA measurements

Because of the high vapour pressure of the Hg chalcogenides the DTA measurements have to be carried out in evacuated sealed quartz ampoules. Cooling and heating curves were measured with different constant rates $R = \mathrm{d}T/\mathrm{d}t$ with $12.5 \geq R/\mathrm{K\,min^{-1}} \geq 2.5$. The measured onset temperatures were extrapolated to $R = 0\,\mathrm{K\,min^{-1}}$. These extrapolated values are shown in Fig. 5 as the transformation temperatures. The melting points of Sb, Zn and HgTe were taken as reference temperatures.

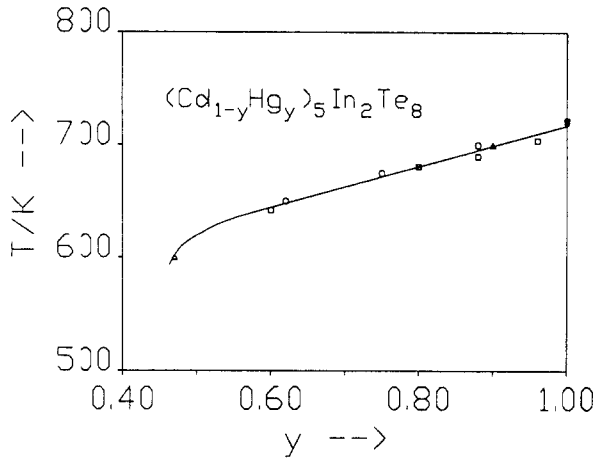

Fig. 5. Transition temperatures of $(Cd_{(1-y)}Hg_y)_5In_2Te_8$ samples as a function of the ratio y: □, as determined from DTA measurements; ○, from electron microprobe analysis; △, from the phase diagrams; •, from Ref. [2].

3. The phase diagram of the quasiternary system $Cd_{(3-3k_2-3k_1)}Hg_{3k_1}In_{2k_2}Te_3$

Results on the phase diagrams of the quasibinary edge systems Hg_3Te_3/In_2Te_3 and Cd_3Te_3/In_2Te_3 have been reported in a previous paper [4].

3.1. Regions of solid solution

Figs. 4(a)–4(g) show several isothermal sections of the phase diagram for the quasiternary system $Cd_{(3-3k_2-3k_1)}Hg_{3k_1}In_{2k_2}Te_3$ as derived from X-ray diffraction and electron microprobe analysis.

Fig. 4(f) shows, for $T = 600$ K, the results of measurements with an electron microprobe on two-phase samples with small spatial extensions of the phase regions. The slopes of the straight lines that characterize the distribution of the composition points measured on equilibrated samples were used to determine the directions of the tie-line fields for the diverse miscibility gaps.

Fig. 4(g) is an example that shows several tie-lines determined from X-ray diffraction measurements by use of the isolattice constant lines and the tie-line directions from Fig. 4(f).

At high temperatures there exist two regions of solid solubility with cubic zincblende structure: one on the (Hg, Cd)Te-rich side (Ia) and the other (Ib) near the In_2Te_3 corner of the phase diagram (cf. Figs. 4(a)–4(d)).

In region Ia the solubility of In_2Te_3 in CdTe-rich alloys is somewhat higher than in HgTe-rich alloys. At 900 K the region Ia extends up to 50–60 mol% In_2Te_3 and its extension decreases with decreasing temperature.

The extension of region Ib is much smaller. Above the order–disorder transition temperature of 890 K, In_2Te_3 can be alloyed with HgTe or CdTe up to some mole per cent (Fig. 4(a)). At lower temperatures in the ordered state of In_2Te_3, however, we could not detect any solubility of CdTe or HgTe in In_2Te_3, and the narrow cubic region Ib is separated from the orthorhombic In_2Te_3 by a miscibility gap that increases rapidly with decreasing temperature. At 700 K the cubic solid solution Ib is restricted to a small region of compositions with a ratio $y > 0.5$ (Fig. 4(d)). At $T = 600$ K the cubic region Ib has totally disappeared (Fig. 4(e)).

There exists a third region of solid solutions (II) that extends from $k_2 = 0.75$ upwards (cf. Figs. 4(a)–4(e)). X-ray patterns of samples belonging to this region show the additional superstructure reflections of the chalcopyrite structure (cf. Fig. 1(c)). A miscibility gap between this tetragonal phase and the In_2Te_3-rich cubic phase Ib could not be detected either by X-ray diffraction or electron microprobe measurements. However, if there were a continuous order–disorder transition between these two regions, one expects that the intensity of the superstructure reflections of the ordered phase would decrease continuously near the boundary between the two regions Ib and II. Instead we observe a rather abrupt disappearance of the superstructure reflections, characterizing an interface between a cubic and a tetragonal phase. Therefore we regard a small miscibility gap between these two regions as more probable than a totally continuous order–disorder transition.

3.2. Ordering phenomena

3.2.1. Near $k_2 = 0.375$

The totally ordered phase. For $T < 720$ K one can observe near $k_2 = 0.375$ (Figs. 4(c), 4(e)) an ordered phase (cf. Fig. 1(b)) with a narrow existence region [2]. This phase (tet1) with stoichiometry $(Cd_{(1-y)}Hg_y)_5In_2Te_8$ extends at $T = 700$ K from $y = 1$ down to $y_c \approx 0.9$ and at $T = 600$ K down to $y_c \approx 0.5$ (cf. Fig. 5). It is separated from the surrounding phase by a miscibility gap that increases with decreasing temperatures.

The partially ordered phase. At $T = 700$ K homogeneous samples outside the miscibility gap also show superstructure reflections of the $Hg_5In_2Te_8$ structure (Fig. 4(c)). Even at higher temperatures (Fig.s 4(a), 4(b)), above the critical point of the low temperature superstructure phase solid solutions yielding superstructure reflections extend on both sides of the composition $k_2 = 0.375$. These partially ordered regions change continuously into the disordered zincblende phase without showing any measurable miscibility gap.

Changes in T. The X-ray patterns of samples with a composition of exactly $k_2 = 0.375$ are largely independent of temperature. Even for samples that were equilibrated at $T = 900$ K one observes the same set of superstructure reflections as for the totally ordered phase that is stable only below $T = 720$ K.

In a previous paper [2] we have shown for the system $Hg_{3-3k_2}In_{2k_2}Te_3$ that at the transition point $k_2 = 0.375$, $T = 720$ K the totally ordered low temperature phase $Hg_5In_2Te_8$ transforms into a partially ordered high temperature phase. Most probably by this transition only the small In ions and structural vacancies become statistically disordered, whereas the large Hg ions retain the arrangement which they already took in the low temperature phase. DTA measurements show that this order–disorder transition is coupled to a thermal effect, as expected for a first order phase transition.

Samples with the ideal molar fraction $k_2 = 0.375$ can be described by $(Cd_{(1-y)}Hg_y)_5In_2Te_8$. DTA measurements on this quasibinary section yield a critical curve $T_c(y)$ for $k_2 = 0.375$ (Fig. 5), which demonstrates that the higher the ratio y the more stable the totally ordered structure.

The electron microprobe analysis of a solid state reaction, carried through at 700 K between a $CdIn_2Te_4$ and a HgTe crystal, yields for the X-ray intensity profile of In at $y \approx 0.93$ an unsteady composition change of $\Delta k_2 \approx 0.06$ near $k_2 = 0.375$. This concentration jump corresponds to the total width of the two miscibility gaps surrounding the completely ordered tetragonal phase. From this result we can estimate for 700 K a critical point at $y_c \approx 0.9$, in good accordance with the above-mentioned DTA measurements.

From the X-ray diffraction measurements at 600 K (cf. Fig. 4(e)) we derive a critical point at $k_{2c} = 0.375$, $y_c \approx 0.47$.

The critical curve plotted in Fig. 5 shows that for $k_2 = 0.375$ an order–disorder transition can be achieved either by increasing the temperature at constant molar fraction y or by decreasing the molar fraction y at constant temperature.

Changes in y. Even if, in the partially ordered solid solutions at $k_2 = 0.375$, the ratio y decreases, the number and intensity of the reflections in the X-ray pattern do not change until rather abruptly near $y \approx 0.5$ all superstructure reflections disappear. Obviously the degree of order in the sublattice of the divalent cations is not only independent of temperature, but also independent of the ratio y as long as a critical Cd content is not exceeded.

Changes in k_2. If the composition of the solid solutions deviates from $k_2 = 0.375$, the X-ray patterns change in so far as, for samples quenched from the equilibration temperature, the sharpness and intensity of the superstructure reflections decrease with increasing distance from the ideal composition $k_2 = 0.375$. At higher distances more and more superstructure reflections disappear until, beyond a certain boundary, only the pattern of the zincblende structure is left. This boundary is characterized in Figs. 4(a)–4(c) by a closed line. We explain this dependence of the intensities on composition as being caused by a continuously decreasing order. This means that the ordered arrangement of the divalent cations, especially that of the big Hg ions, becomes more unstable the more the ratio of trivalent to divalent cations deviates from 2:5.

3.2.2. Near $k_2 = 1$

According to our DTA measurements and to X-ray investigations on quenched samples [5], pure In_2Te_3 undergoes an order–disorder transition at $T \approx 890$ K. Other data in the literature range between 853 K [6] and 903 K [7]. Whereas the ordered cubic high temperature phase forms solid solutions with CdTe and HgTe, the orthorhombic low temperature phase does not show any detectable solubility for the II–VI components.

Most probably the differences in cationic radii are not decisive for this behaviour; for In_2Te_3 can be alloyed with considerable amounts of the isovalent Ga_2Te_3 without preventing the ordering transition, though the ratio $r_{In^{3+}}/r_{Ga^{3+}} = 1.48$ deviates distinctly more from 1 than the ratio $r_{In^{3+}}/r_{Cd^{2+}} = 0.89$ [8]. But, for every two In cations that are exchanged by three divalent cations one structural vacancy must vanish. Obviously the ordering process demands rather exactly that one third of the sites in the cationic sublattice of the zincblende structure be vacant.

3.3. Miscibility gaps

Owing to the existence of ordered phases, the phase diagram shows several structural miscibility gaps, especially between the ordered phases and the surrounding disordered cubic phase, but also between different ordered phases.

3.3.1. Miscibility gaps between ordered phases

For example, at 600 K there is a miscibility gap between the chalcopyrite phase (tet2) and the ordered phase (tet1) (cf. Figs. 4(e)–4(g)). This two-phase region (tet2/tet1) is neighboured by two three-phase regions (tet2/tet1/cub), each including a disordered cubic phase with zincblende structure. The existence of the very tiny cubic region near the Hg_3Te_3/In_2Te_3 edge was detected from the X-ray patterns of one three-phase sample and several samples of the adjacent two-phase regions (tet2/tet1). From the cubic reflection sets of all these samples we calculated values for the cubic lattice constant in the range $629.3 \leq a_{cub}/\text{pm} \leq 630.3$. Using Eq. (1) we derived from these data

an extension of this cubic phase on the Hg_3Te_3/In_2Te_3 edge of $0.47 \leq k_2 \leq 0.51$. At lower temperatures this small island of the cubic phase will disappear together with the adjacent three-phase region (cf. Ref. [9]).

Another miscibility gap (orh/tet2) between ordered phases extends at 600 K between the orthorhombic In_2Te_3 phase and the chalcopyrite phase. On the Hg_3Te_3/In_2Te_3 edge, somewhere between 650 and 700 K, there must be a eutectoidic point (orh/cub/tet2) at which a disordered cubic phase is formed in equilibrium with the tetragonal chalcopyrite phase and the orthorhombic In_2Te_3 (cf. Fig. 4(d) and Ref. [4]). On the Cd_3Te_3/In_2Te_3 edge the corresponding eutectoidic point arises somewhat above 700 K [4]. Thus, at 700 K a three-phase region (orh/cub/tet2) separates a Cd chalcogenide rich two-phase region (orh/tet2) from the two-phase region (orh/cub), which is restricted to the region $y > 0.4$ and disappears at higher temperatures.

3.3.2. Spinodal miscibility gaps

Moreover, in the quasiternary section for 600 K (Figs. 4(e)–4(g)) a spinodal miscibility gap extends from the quasibinary edge Cd_3Te_3/In_2Te_3 into the CdTe rich cubic phase. For this spinodal miscibility gap the critical curve, beyond which the disordered cubic phase is stable, runs from the point ($k_1 = 0$, $k_2 \approx 0.2$, $T \approx 680$ K) to the point ($k_1 \approx 0.23$, $k_2 \approx 0.15$, $T = 600$ K). Just at 600 K the system on the quasibinary edge Cd_3Te_3/In_2Te_3 reaches a eutectoidic point (cub/cub/tet2) [4], where the two cubic phases are in equilibrium with the tetragonal chalcopyrite phase. Because of the extremely long times needed for equilibration at low temperatures, we could not realize the establishment of equilibria below this eutectoidic temperature. Nevertheless, we can conclude that below 600 K a structural miscibility gap must extend from nearly pure CdTe up to the chalcopyrite phase. This causes the spinodal miscibility gap to detach from the quasibinary edge and to move with decreasing temperature more and more into the quasiternary region. Thus, in analogy to observations reported in Ref. [1], a three-phase region between the chalcopyrite phase and the two cubic regions must arise below 600 K.

Within the tetragonal phase (tet2) no miscibility gap could be detected by X-ray diffraction measurements. Nevertheless, a spinodal miscibility gap must also occur within this phase (cf. Fig.s 4(a)–4(c)), since in samples that were annealed in the region $700 \leq T/K \leq 900$ such a two-phase region could be detected from X-ray intensity profiles measured with an electron microprobe. Within the quasiternary region of the chalcopyrite phase the reaction path for a reaction between an In_2Te_3 and a $Cd_{1/2}Hg_{1/2}In_2Te_4$ crystal yields a concentration step between two regions of equal structure but different composition. Thus, we are sure that for $T \leq 850$ K the whole region of the tetragonal chalcopyrite phase is separated into two parts by a spinodal miscibility gap with a width of $\Delta k_2 \approx 0.04$. On the quasibinary edge Hg_3Te_3/In_2Te_3 the spinodal miscibility gap could only be detected in profiles for 700 and 800 K, but not for 900 K. Thus, on this edge of the phase diagram the critical point of the spinodal miscibility gap ranges somewhere between 800 and 900 K.

Acknowledgements

Financial support of this work by the Deutsche Forschungsgemeinschaft and the Fonds der Chemischen Industrie is acknowledged.

References

[1] A. Zeppenfeld and V. Leute, *Ber. Bunsenges. Phys. Chem.*, *96* (1992) 1558–1564.
[2] V. Leute and H.M. Schmidtke, *J. Phys. Chem. Solids*, *49* (1988) 409–420.
[3] V. Leute, *Ber. Bunsenges. Phys. Chem.*, *95* (1991) 713–720.
[4] D. Weitze and V. Leute, *J. Alloys Comp.*, in press.
[5] V. Leute and U. Spalthoff, *Forschungsberichte des Landes Nordrhein-Westfalen*, Nr. 2914, Westdeutscher Verlag, 1979.
[6] P.G. Rustamov, Y.N. Nasirov, M.A. Alidzhanov and Y.N. Babaey, *Inorg. Mater.*, *13* (1977) 608.
[7] J.C. Woolley, B. Pamplin and P.J. Holmes, *J. Less-Common Met.*, *1* (1959) 362.
[8] J. Emsley, *The elements*, Clarendon Press, Oxford, 1989.
[9] V. Leute and H.M. Schmidtke, *J. Phys. Chem. Solids*, *49* (1988) 1317–1327.